Correspondence: David Martínez-Torres, Institut de Biologia Integrativa de Sistemes. Parc Cientific Universitat de Valencia C/ Catedrático José Beltrán nº 2, 46980 Paterna, València, Spain. Tel: +34 963 543 644. Email: david.martinez@uv.es

ORIGINAL ARTICLE

Melatonin in the seasonal response of the aphid *Acyrthosiphon pisum*

Miquel Barberà[1], Laura Escrivá[1], Jorge Mariano Collantes-Alegre[2], Giuseppe Meca[2], Ezio Rosato[3] and David Martínez-Torres[1]

[1]*Institut de Biologia Integrativa de Sistemes & Institut Cavanilles de Biodiversitat i Biologia Evolutiva; Parc Cientific Universitat de Valencia; C/ Catedrático José Beltrán nº 2; 46980 Paterna; València; Spain;*
[2]*Laboratory of Food Chemistry and Toxicology, Faculty of Pharmacy, Universitat de València, Burjassot, Spain;*
[3]*Department of Genetics, University of Leicester, Leicester LE1 7RH, UK*

Abstract

Aphids display life cycles largely determined by the photoperiod. During the warm long-day seasons, most aphid species reproduce by viviparous parthenogenesis. The shortening of the photoperiod in autumn induces a switch to sexual reproduction. Males and sexual females mate to produce overwintering resistant eggs. In addition to this full life cycle (holocycle), there are anholocyclic lineages that do not respond to changes in photoperiod and reproduce

This is an Accepted Article that has been peer-reviewed and approved for publication in the Insect Science but has yet to undergo copy-editing and proof correction. Please cite this article as doi: 10.1111/1744-7917.12652.

continuously by parthenogenesis. The molecular or hormonal events that trigger the seasonal response (i.e. induction of the sexual phenotypes) are still unknown. Although circadian synthesis of melatonin is known to play a key role in vertebrate photoperiodism, the involvement of the circadian clock and/or of the hormone melatonin in insect seasonal responses is not so well established. Here we show that melatonin levels in the aphid *Acyrthosiphon pisum* are significantly higher in holocyclic aphids reared under short days than under long days, while no differences were found between anholocyclic aphids under the same conditions. We also found that melatonin is localised in the aphid suboesophageal ganglion (SOG) and in the thoracic ganglionic mass (TGM). In analogy to vertebrates, insect-type arylalkylamine *N*-Acetyltransferases (i-AANATs) are thought to play a key role in melatonin synthesis. We measured the expression of four *i-AANAT* genes identified in *A. pisum* and localised two of them *in situ* in the insect central nervous systems (CNS). Levels of expression of these genes were compatible with the quantities of melatonin observed. Moreover, like melatonin, expression of these genes was found in the SOG and the TGM.

Key words AANAT; aphid; *in situ* hybridization; melatonin; photoperiodism; quantification

Introduction

Aphids (Hemiptera: Aphididae) are insects sucking plant sap that display complex life cycles characterised by cyclical parthenogenesis. The typical aphid life-cycle consists of viviparous succession of several parthenogenetic generations during the plants' growing seasons, alternating with a single sexual generation induced by short photoperiod which serves as a token of the arrival of winter. Males and sexual (oviparous) females mate and lay winter eggs that hatch in spring giving rise to the first generation of parthenogenetic reproduction. Thus, short photoperiods induce sexual reproduction in which the eggs enter diapause. Alongside the holocyclic life-cycle there are naturally occurring anholocyclic aphid lineages within species

(or even whole species) that do not respond to changes in photoperiod and reproduce parthenogenetically all year round. In a way, these could be considered life-cycle mutants. This type of incomplete cycle tends to evolve in regions with mild winters, where parthenogenetic females can survive the unfavourable (but temperate) season. In dioecious species, in which the sexual and parthenogenetic morphs use alternative hosts (primary and secondary hosts respectively), anholocyclic lineages may also arise in regions where the primary host plant is absent (Moran, 1992). Since photoperiod is the main cue used in most aphids to trigger the sexual response, they are considered paradigmatic photoperiodic insects. Indeed, photoperiodism was first reported in animals in the aphid *Megoura viciae* (Marcovitch, 1924).

The transduction of the photoperiodic signal has been best characterised in vertebrates. In mammals, involvement of the circadian clock in photoperiodism is well established (Wood & Loudon, 2014). Indeed, photoperiodic information perceived by photoreceptors located in the retina is transduced to the suprachiasmatic nucleus (SCN) in the hypothalamus where the central pacemaker of the circadian system resides (Dibner *et al*., 2010; Lucas, 2013). A crucial element in mammalian photoperiodism is the circadian synthesis of melatonin in the pineal gland. This is under control of the SCN by means of circadian regulation of arylalkylamine *N*-acetyltransferase (AANAT), the rate limiting enzyme in melatonin biosynthesis (Klein, 2007; Cazaméa-Catalan *et al*., 2014; Wood & Loudon, 2014). Melatonin levels exhibit a daily rhythm driven by the circadian clock, with plasma levels high at night (hence the name, hormone of darkness) and low during the day (Lincoln, 2006). Information on the length of the day is encoded by the melatonin signal, with longer or shorter nights yielding extended or shortened melatonin messages in autumn and spring respectively (Lincoln, 2006; Dardente *et al*., 2010).

Such signals alternatively activate the molecular pathways that lead to winter or summer responses (e.g. reproduction, migration, hibernation, etc.). Vertebrate AANATs (vAANATs) belong to a family of proteins (the Gcn5-related *N*-acetyltransferases or GNAT family) that catalyse a transacetylation reaction from acetyl coenzyme A to different substrates (Vetting *et al*., 2005). For melatonin synthesis, AANAT specifically acetylates serotonin thus yielding *N*-acetyl serotonin, which is the immediate precursor of melatonin (Hardeland, 2010). AANAT activity increases 10- to 100-fold during the night, leading to the observed rhythmicity in melatonin levels. Given its unique role in time keeping, vAANAT has been regarded as the Timezyme (Klein, 2007).

The study of photoperiodism in insects has been characterised by the controversy on whether the circadian clock plays a central role in the regulation of the seasonal response or if, on the contrary, it is controlled by an hourglass-like system in which no circadian oscillator is involved (Saunders, 2010). In recent years, evidence that circadian clock genes participate in the photoperiodic response has accumulated for different insect species (Pavelka *et al*., 2003; Sakamoto *et al*., 2009; Ikeno *et al*., 2010, 2011a, 2011b, 2013; Mohamed *et al*., 2014; Pegoraro *et al*., 2014; Meuti *et al*., 2015). Nevertheless, some authors claim that such results should be taken cautiously, because pleiotropic effects (i.e. clock-independent roles of particular clock genes) could lead to misleading conclusions (Bradshaw & Holzapfel, 2007, 2010; Emerson *et al*., 2009a, 2009b). In this respect, novel experiments in *Drosophila* analysed the effect of several clock mutants in the seasonal response and showed that the circadian clock is involved in photoperiodic time measurement as a whole (Pegoraro *et al*., 2014). Back to melatonin, this molecule has been detected and quantified in many invertebrates. The majority of insects for which melatonin has been quantified show higher levels at night (Vivien-Roels & Pévet, 1993; Gorbet & Steel, 2003; Bembenek *et al*., 2005; Vieira *et al*., 2005; Yang *et al*., 2007; Mohamed

et al., 2014), as in mammals. In particular, melatonin has been found to participate in the seasonal response in the lepidopteran *Antheraea pernyi* (Wang *et al*., 2013; Mohamed *et al*., 2014). Thus, current evidence suggests a conserved role for melatonin as a hormone of darkness also in insects, although a role as a conveyor of circadian oscillation throughout the organism is not that clear (Gao & Hardie, 1997; Niva & Takeda, 2003; Mohamed *et al*., 2014; Wang *et al*., 2015; Kamruzzaman *et al*., 2016). However, exogenous melatonin has been found to lead to more synchronized locomotor activities in arrhythmic insects (Yamano *et al*., 2001).

Although generally assumed to be similar to vertebrates, it is not fully demonstrated that melatonin biosynthesis in arthropods proceeds through the same pathway, including the conversion of serotonin into *N*-acetyl serotonin by an arylalkylamine *N*-acetyltransferase. In fact, insects lack orthologues of vertebrate AANAT (v-AANAT) but instead contain insect-specific AANATs (i-AANATs) that are assumed to play an equivalent role in melatonin biosynthesis. Recently, it has been shown in *Antheraea pernyi* that i-AANAT controls melatonin levels under the regulation of the circadian clock (Mohamed *et al*., 2014).

The pea aphid *Acyrthosiphon pisum* has been established as a model species and its genome has been sequenced and made publicly available (The International Aphid Genomics Consortium, 2010). It displays the typical aphid life cycle described above and both holocyclic and anholocyclic lineages are available. Thus it is an excellent system to investigate the molecular mechanisms governing photoperiodism in aphids and more generally in insects. Previous studies have shown that melatonin fed pea aphids are partially induced to develop sexual morphs under summer-like photoperiod, suggesting a role for this hormone in triggering the seasonal response (Gao & Hardie, 1997). Moreover, we have identified and characterised four i-AANAT coding genes in the pea aphid genome and for three of them shown higher expression under short photoperiod conditions (Barberà *et al*., 2013). In the present report, we

have investigated the role of melatonin in the photoperiodic response in the pea aphid *A. pisum*. We report data on melatonin quantification in individuals reared under long-day or short-day conditions, both in a holocyclic and an anholocyclic strain. In addition, for the first time in aphids and in a hemimetabolous insect, we show the putative localisation of melatonin in central nervous system.

Materials and methods

Aphid rearing

Two strains of the pea aphid *Acyrthosiphon pisum* were used in the experiments: York Red 2 (YR2) and Gallur Rojo (GR), originally collected in York (UK) and Gallur (Spain), respectively. The first is our holocyclic reference strain and has a canonical seasonal response (i.e. sexual morphs are produced under short photoperiods). The latter is our anholocyclic reference strain, which continues reproducing through parthenogenesis independently of photoperiodic conditions. Both strains have been kept in our lab under long day conditions (i.e. 16L : 8D) at 18ºC as parthenogenetic clones on *Vicia faba* for more than 10 years.

To guarantee that aphids used were all of the desired age, we synchronised aphid colonies by founding them using aphids born during a 6–8 hours interval. Synchronised aphids of the L3 stage were split in two groups (Fig. S1). One group, referred to as LD G0, was kept under long day (LD) conditions. The second group was transferred to short day (SD) conditions (i.e. 12L : 12D), thus named SD G0. The next generation of aphids born under SD conditions from SD G0 individuals was named SD G1. In parallel, LD G1 aphids were obtained similarly but under LD conditions. Aphids collected for the different experiments were either snap-frozen and kept at –70ºC until used or fixed (see below). Figure S1 summarises aphid ages and their processing

previous to each type of experiment. For RNA extraction and melatonin quantification LD G1 and SD G1 adult aphids were collected by snap-freezing them in liquid nitrogen and stored at –70ºC. Induction of the seasonal response was confirmed by checking the presence of males and sexual females in the G2 progeny born from SD G1 aphids. In all cases, aphids of the holocyclic strain (YR2) always produced sexual morphs under SD photoperiod while aphids of the anholocyclic strain (GR) kept reproducing parthenogenetically.

Aphid fixation and dissection

Aphids were fixed in PFAT-DMSO (4% paraformaldehyde in 1× PBS, 0.1% TritonX-100, 5% DMSO v/v) over night at 4ºC. Fixed individuals were washed 3 × 10 min in PBSTx (TritonX-100 0.1% in 1× PBS). Subsequently, dissections were carried out in glass block dishes on ice in cold PBSTx. The head capsules were carefully opened with tweezers and the CNS, including the brain and ganglia, were dissected out. From this point, CNSs that were going to be used only for melatonin localisation were pooled in cold PBTx, immediately proceeding to its detection using the corresponding antibody. CNS to be used in mRNA localisation by *in situ* hybridisation (ISH) were pooled in ice cold methanol immediately after dissection, washed twice in methanol, and stored at –20ºC in tight sealed microcentrifuge tubes until the ISH protocol was initiated.

Melatonin localisation

Individuals from both YR2 and GR pea aphid strains were collected at ZTs 3–6 from long day (LD) and short day (SD) conditions (see above and Fig. S1). Sampling included aphids from the four larval stages and up to 9 days old adults for each strain and photoperiod. All CNSs were fixed and dissected as described in the previous section. Afterwards, CNSs were pre-incubated overnight at 4ºC in blocking solution containing PBS, 0.5%, TritonX-100, 10%

Normal Goat Serum (NGS, Sigma Aldrich). Next, CNSs were incubated in 1 : 300 rabbit anti-melatonin antibody (Byorbit, UK) diluted in 10% NGS, 0.1% sodium azide and PBST 0.5%, for 5 days at 4ºC. The excess, non-specifically bound antibody was then removed by washing CNSs for 10 min in PBST 0.1% three times. Detection with a secondary antibody was carried out by incubating with Cy3 goat anti-rabbit 1 : 300 (Jackson Immunoresearch, UK) in 10% NGS, 0.1% sodium azide and PBST 0.5% for 1–2 days at 4ºC. The excess, unspecifically bound secondary antibody was removed by washing CNSs for 10 min in PBST 0.1% three times. Finally, CNSs were mounted on microscope glass slides with glycerol containing 3% propyl gallate. To check the specificity of the primary antibody, brain preparations of larval stage of *Brithys crini* and late stage pupae of *Spodoptera exigua* were included as controls both producing positive signal exclusively localised in two pairs of cells equivalent to those reported by Mohamed *et al*. (2014) in the only insect where melatonin has been *in situ* localised until now, the Chinese oak silkmoth (Fig. S2 A and B). In addition, a control incubation without the primary antibody was included. (Fig. S2C).

Melatonin detection and quantification by HPLC-MS/MS

Melatonin extraction from insects was carried out on ice under dark conditions to prevent degradation. The aphids were introduced into 2 mL tubes (wrapped in aluminium foil) and 0.5 mL of methanol/water 1 : 1 (v/v) were added. The samples were completely homogenised using an Ultraturrax T8 IKA (Staufen, Germany) during 1 min and centrifuged at 14 000 r/min at 4 ºC for 10 min. The supernatant fraction was filtered through a 0.22 μm filter Phenomenex (Madrid, Spain) and 10 μL were injected into a liquid chromatography-tandem mass spectrometry (HPLC-MS/MS) system.

Quantification of melatonin content was carried out following a method specifically developed for aphids (Escrivá *et al*., 2016). Three replicate groups of 50 adult aphids from the

two strains and both LD and SD photoperiods were sampled and accurately weighted at two different moments along the day-night cycle (i.e., ZT6 and ZT18, that is, 6 and 18 hours after lights on, respectively). The insects were snap frozen in liquid nitrogen and stored at –80ºC until melatonin extraction.

Analysis of expression of AANAT genes by RT-qPCR

Real time quantitative PCR (RT-qPCR) was used to quantify the expression of the four *i-AANAT* genes previously identified (Barberà *et al*., 2013) using the primers shown in Table S1 in heads of G1 aphids of the YR2 and GR strains reared under LD and SD conditions. Differently from the previously reported study (Barberà *et al*., 2013), in the present study, expression of i-AANAT genes was analysed at 6 timepoints covering 1.5 days and only in two aphid categories (LD and SD aphids of the G1 generation). Most relevant, in the present study, expression of genes is compared between holocyclic and anholocyclic aphids (strains YR2 and GR respectively). For each condition and strain, aphids were sampled at six different moments along the day/night cycle starting 3 h after lights on and collected at 6 h intervals (ZT3, ZT9, ZT15, ZT21, and ZT3 and ZT9 in the second day). The samples were immediately frozen in liquid nitrogen and kept at −70°C until RNA extraction. RNA extraction, cDNA synthesis and RT-qPCR were performed as described in Barberà *et al*. (2013). Relative expression for each sample was calculated using the $\Delta\Delta C_T$ (threshold cycle) method (Livak & Schmittgen, 2001) on values normalised to a reference sample used in all experiments (inter-run calibrator). Differences between mean expression values of the variables strain, rearing photoperiod and moment of the day/night cycle, were tested for statistical significance using ANOVA. In addition, homogeneity of variances was assessed by Levene tests. HSD Tukey and Bonferroni *post hoc* tests were applied when variances were homogeneous, and Games-Howell *post hoc*

analyses when variances were not homogeneous. All statistical tests were performed using the SPSS Statistics package v22.0 software (IBM Corp). When ANOVA tests revealed significant differences in expression between ZTs, a COSINOR analysis (Refinetti *et al*., 2007; Cornelissen, 2014) was performed to test for circadian rhythmicity.

RNA probe synthesis

RNA probes labelled with digoxigenin (DIG) were synthesised by a modification of the method described by Wülbeck and Helfrich-Förster (2007). First, cDNA regions of each gene of interest of approximately 600 to 900 bp were amplified by PCR (Tables S1 and S2). PCR products were purified by ammonium precipitation and the amplicon size was checked by electrophoresis on agarose gels. Next, the purified PCR product was cloned into pGEM®-T easy vector (Promega) and used to transform DH5α *Escherichia coli* competent cells (Life Technologies). Then, colony PCR was used to screen for transformants with the appropriate inserts and those that revealed positive, were purified and sequenced from both extremes using SP6 and T7 primers to know the orientation of the insert. Subsequently, minipreps of selected colonies were performed to obtain purified insert-containing plasmids using High Pure Plasmid Isolation Kit (Roche). To synthesise the riboprobes, templates were obtained by simply doing a PCR with SP6 and T7 primers (Table S1) and DNA fragment purification with the High Pure PCR Product Purification Kit (Roche). The purified PCR products were then quantified by spectrophotometry using a NanoDrop ND-1000 (Nanodrop Technologies, Inc., Wilmington, DE, USA) and used as a template for RNA transcription. Taking into account the insert orientation, purified templates were used to synthesise DIG-labelled sense and antisense probes with RNApol SP6 or RNApol T7 (both from Roche). Sense probes were used as negative controls. Antisense probes were used to localise gene specific mRNAs. Transcription

was carried out on 200 ng DNA template in 0.2 mL microcentrifuge tubes following the vendor recommendations (Roche). To stop the reaction, 2 μL of 0.2 M EDTA pH 8.0 were added and the reaction was stored at 4ºC until purification. Probes were purified with mini QuickSpin RNA columns (Roche) following the manufacturer's instructions, diluted 50% with deionised formamide and stored at –20ºC until use.

Localisation of AANAT transcripts by RNA in situ hybridisation

Localisation of transcripts was carried out using DIG-labelled RNA probes (see above). Fixed CNSs (see above) stored in 100% methanol were gradually rehydrated in PBTw (0.1% Tween 20 in RNase free 1× PBS), washed in PBTw, and treated with proteinase K (3 μg/mL) for 3 min at room temperature and 1 h on ice. Proteinase digestion was blocked with 2 mg/mL glycine. Next, CNSs were refixed in PFATw (4% para-formaldehyde in 1× PBS, 0.1% Tween 20) for 20 min and washed 5 times in RNase free PBTw for 5 min each. Then, the samples were incubated for 5 min in a 1 : 1 mix of PBTw and pre-hybridisation buffer (preHB; 5× SSC (saline sodium citrate), 50% formamide, and 0.1% Tween 20). Blocking was carried out by incubating for 2 h on a water bath at 65ºC in hybridisation buffer (HB; preHB plus 100 μg/mL heparin, 100 μg/mL salmon sperm DNA and 500 μg/mL yeast tRNA, pH 6.0). Next, the blocked CNSs were hybridised by incubating with HB plus the corresponding probe overnight at 65ºC in a water bath. Non-specifically hybridised probe was removed with the following washes at 65ºC: two washes of 15 min in preHB, three washes of 15 min each in increasing mixes of preHB:2× SSC with 0.1% Tween 20 (3 : 2, 1 : 1, 2 : 3), a single wash of 15 min in 2× SSC with 0.1% Tween 20, followed by two washes of 15 min in 0.2× SSC with 0.1% Tween 20. At this point, the following washes were carried out at room temperature: three washes of 10 min each in increasing mixes of 0.2× SSC with 0.1% Tween 20: PBTw transition (3 : 2, 1 :

1, 2 : 3), and three washes of 5 min in PBTw. Next, CNSs were blocked by incubation for 2 h in PBTw supplemented with 1% Blocking Reagent (Roche) at room temperature with gentle shaking. Afterwards, the blocking buffer was replaced with fresh blocking buffer plus 1:1000 AP-conjugated anti-DIG Fab fragments (Roche) and incubated overnight at 4ºC with gentle shaking. Fast Red/HNPP that produces a chromogenic red and fluorescent precipitate (both from Roche) was used as AP substrate following the manufacturer's instructions. The reaction was stopped by washing three times for 5 min in PBTw.

Colocalisation of transcripts and melatonin

Colocalisation of the aphid insect-type AANAT transcripts and melatonin was achieved by combining ISH and melatonin detection using antibodies previously described. First, the RNA ISH protocol was applied as described above, except that especial care was taken to protect samples from light to avoid photo-degradation of melatonin (Brömme *et al*., 2008). After the last wash in PBTw, the tissues were transferred to the blocking step of the Melatonin localisation (see above). To avoid interference of fluorescent signal detection between the secondary antibody Cy3 goat anti-rabbit used for melatonin detection and the AP substrate Fast Red/HNPP, the secondary antibody was replaced by an Alexa647 goat anti-rabbit.

Microscopy and imaging

Whole-mount fluorescent preparations of the CNS were scanned with a confocal laser scanning microscope (FV1000, Olympus) using 20× and 40× objectives. All brains were scanned with a scanning speed of 400 or 200 Hz, a pinhole of 1 Airy unit, a step size of 1.0–0.4 μm, and a line average of 2–4. Kalman filter was activated to remove noise signal. Colocalisation of aphid i-*AANAT* transcripts with melatonin were imaged with 559 nm and 635 nm lasers, respectively. Images were processed and arranged with Fiji v1.50i software (Schindelin *et al*., 2012).

Results

Localisation of melatonin in the aphid CNS

Figure 1 shows the localisation of melatonin-like immuno-histochemical reactivity (MEL-ir) in the aphid central nervous system (CNS). The specificity of the MEL signal was confirmed by the absence of signal in control preparations and by the positive signal produced in the expected brain cells of two Lepidoptera species used as positive controls (see Materials and methods and Fig. S2). In order to investigate the possible changes in MEL distribution along aphid development, CNSs from first instar aphid larvae to 9 days old adults were used for MEL localisation (Fig. 1A). In most preparations, a total of 22 MEL-ir neurons were detected located in the dorsal soma cortex of both the suboesophageal ganglion (SOG) and the thoracic ganglionic mass (TGM) (Fig. 1A). The SOG contains eight MEL-ir neurons distributed in four pairs, (i.e. one pair per hemineuromere or two pairs per segment, Fig. 1A). In the TGM there were a total of 14 MEL-ir neurons arranged in six pairs plus two unpaired neurons (Fig. 1A), in a distribution similar to that seen in the SOG. Each of the thoracic neuromeres included two

pairs of MEL-ir neurons, each pair located on each side of the three thoracic segments. The two unpaired MEL-ir neurons at the posterior part of the TGM correspond to the fused abdominal ganglia (Fig. 1A) (Niven *et al*., 2008). MEL was found mainly in the cytoplasm of the neuron soma, but not in the nucleus (Fig. 1A). In fact, the nucleus of MEL-ir neurons could be discerned by the absence of signal, giving the cell a characteristic doughnut-like shape. The comparison of MEL immunoreactivity in aphid CNSs from the first (L1) to the third larval instar (L3) revealed that MEL was already present in the axonic cones of neurons from the three first larval instars. An evident mobilisation of MEL from the cell bodies to the axons was usually seen from L3 onwards (Fig. 1A). From each pair of MEL-ir neurons in the SOG, two axons run together towards the ventro-medial commissure from where they cross with the axons of the pair of MEL-ir neurons of the opposite hemineuromere. From this point, the axons continued dorsally following the boundary between the soma cortex and the underlying contra-lateral neuropil. Axons of MEL-ir neurons, probably from the SOG, reach the *protocerebrum* (Fig. 1D–E). In adult aphids, these axons form varicosities, and innervations that are terminated in the protocerebral neuropil (Fig. 1D–E). Each of the axons further branched in two secondary processes: one reached the ventral region innervating the *tritocerebrum*, while the other continued ventrally in the *protocerebrum* turning upwards in the frontal region finally innervating the *pars lateralis* (Fig. 1D–E).

With respect to the MEL-ir in the thoracic ganglia (T1, T2 and T3), the axonic pattern was similar to that described for the MEL-ir in the SOG. From each pair of neurons, two axons extended to the ventro-medial commissure (Fig. 1B, full arrowheads), where they cross with the MEL axons from the contra-lateral hemineuromere in the same way they did in the SOG. From that point, one of the processes continued to the posterior distal part of the contra-lateral hemiganglion, where the axon adopted an arc-shaped form while turned dorsally (Fig. 1D,

empty arrowheads). The final segment of the axon extended further forming an arborised region in the dorsal neuropil (Fig. 1B–C).

The two unpaired MEL-ir neurons corresponding to the abdominal ganglia (Fig. 1A) projected axons to the posterior ventro-medial region. From there, the axons sharply turned dorsally and then ran in parallel to the posterior part of the ganglia, probably extending into the posterior nerve (Fig. 1A and C). In the adult stage of development, the neurites of all MEL-ir neurons in the SOG shared a striking feature, namely the appearance of swellings or varicosities followed by arborisations along the processes (Fig. 1A–E), including the processes reaching the *protocerebrum* (Fig. 1D–E). In the oldest aphids (A9 in Fig. 1A), the soma of MEL-ir neurons was virtually devoid of melatonin, being present only in the axons.

The previously described distribution and mobilisation of MEL in developmental time was compared in aphids from the holocyclic (YR2) and the anholocyclic (GR) strains (data not shown). For each strain aphids reared under LD (Long Day) and SD (Short Day) conditions were included. No major differences were observed in the number or distribution of MEL-in or in the timing of MEL mobilisation.

Quantification of melatonin content

Melatonin was both detected and quantified in whole adult aphids following an HPLC-MS/MS method previously developed for aphid samples (Escrivá *et al*., 2016). In order to reveal a possible involvement of melatonin in the aphid seasonal response, the quantification was carried out in aphids of the holocyclic and anholocyclic strains reared under LD and SD photoperiods. To detect daily differences in putative melatonin titre, two time points of the day/night cycle (ZT6 and ZT18) were analysed for each strain and photoperiod. Figure 2 (see also Table S3) shows these results. Most relevant, aphids of the holocyclic strain (YR2) reared

under SD conditions showed significantly higher content at the two time points analysed than those reared under LD photoperiod (Fig. 2B). Contrarily, for the anholocyclic strain (GR), melatonin levels were not significantly different between the two photoperiods (Fig. 2B). Moreover, melatonin levels in GR aphids reared under both photoperiods were similar to those observed in the YR2 strain reared in LD (Fig. 2B). Finally, no significant differences were found in MEL levels between the two ZTs in any strain or photoperiod analysed (Fig. 2A).

Quantification of AANAT *expression in aphid heads*

Although differences in transcript levels among different ZTs were observed for the different i-AANAT genes analysed, COSINOR analysis, only revealed significant rhythmicity in the expression of some genes under particular photoperiods in the GR strain (Fig. S3). Comparison of global expression levels of the four aphid i-AANATs showed that *AANAT1* was most highly expressed, followed by *AANAT2, AANAT3* and *AANAT4*, in that order (Fig. 3). Higher expression in SD respect to LD in YR2 aphids was observed for *AANAT1*, *AANAT2* and *AANAT3*, (see Fig. 3). On the other hand, for the anholocyclic GR strain *AANAT1*, *AANAT2* and *AANAT4* showed significantly higher expression in SD with respect to LD.

Localisation of AANAT transcripts and melatonin

In order to investigate, though indirectly, if any of the four aphid i-*AANAT* genes could be considered a candidate to be involved in melatonin synthesis, we attempted to localise their transcripts by *in situ* hybridisations and to compare the results with those obtained for melatonin localisation (see above). Only transcripts corresponding to aphid *AANAT2* and *AANAT3* genes yielded positive results after *in situ* experiments in CNSs of L3 and adult aphids of the YR2 strain (Figs. S4 and 4, respectively). The specificity of the probes was

confirmed by the absence of staining in preparations in which the respective sense probes used. CNSs hybridised with sense and antisense probes showed tracheal non-specific staining (e.g. see Fig. 4A). Similar to melatonin localisation, expression of *AANAT2* was restricted to the ganglia (Fig. 4A, C), in which several cells distributed in a similar pattern to that for melatonin neurons was observed (Fig. 4B). However, the position and number of neurons expressing *AANAT2* was different from those that showed melatonin immunoreactivity. The SOG contained four strongly stained neurons expressing *AANAT2* located at the anterior region, close to the circumoesophageal connective between SOG and the brain (Fig. 4A). Additionally, five dorsal clusters each containing approximately four neurons were found in the antero-medial region of neuromeres S1, S2, T1, T2, and T3 (Fig. 4A). It thus seemed that each pair of melatonin neurons was associated to two *AANAT2* neurons, except the abdominal group that was associated to two neurons (Fig. 4C). In summary, 26 *AANAT2* expressing neurons were identified in the aphid CNS: the SOG contained four anterior and eight dorsal neurons, while the TGM contained a total of 16 neurons expressing *AANAT2*. Differently to *AANAT2*, expression of *AANAT3* was observed in a larger number of neurons (Fig. 4D), distributed in all three parts of the CNS, including the *protocerebrum* and optic lobes, the and the TGM. Despite the great number of *AANAT3* expressing neurons, none of them colocalised with melatonin neurons (Fig. 4D–F). Generally, the *AANAT3* neurons were found in a deeper position of the soma cortex, closer to the underlying neuropil. *In situ* were also carried out with probes against *AANAT1* and *AANAT4*. Unfortunately, no specific staining was observed for these two genes.

Discussion

In this study, we have described for the first time in aphids (and in hemimetabolous insects) the putative sites of melatonin synthesis in the nervous system as well as the dynamics of its distribution through development. Additionally, we have compared levels of melatonin in two aphid strains displaying alternative life-cycles reared under short or long photoperiods. Finally, to test if any of the four aphid i-AANATs described could be involved in melatonin synthesis we have *in situ* localised them and quantified their expression in aphid heads.

In mammals, melatonin is known to be the principal endocrine factor in output pathway of circadian rhythms as well as a photoperiodic token (Dardente *et al*., 2010; Wood & Loudon, 2014). Its synthesis by the pineal gland is controlled by specific AANATs whose expression is under control of the central circadian clock that resides in the suprachiasmatic nucleus of the hypothalamus (Lincoln, 2006; Ikegami & Yoshimura, 2012). In insects, however, the role of melatonin in circadian and seasonal rhythms has been less investigated. Nevertheless, some studies have shown that the levels of melatonin and AANAT enzymatic activity correlate in different tissues, including the insect brain and haemolymph (Itoh *et al*., 1995; Itoh & Sumi, 1998; Vieira *et al*., 2005; Mohamed *et al*., 2014). Additionally, the quantification of melatonin in some insect species revealed higher levels in the dark as in vertebrates (Vivien-Roels & Pévet, 1993; Gorbet & Steel, 2003; Bembenek *et al*., 2005; Vieira *et al*., 2005; Yang *et al*., 2007; Mohamed *et al*., 2014). However, the biosynthetic pathway for melatonin production is not well-known in insects. They lack true vertebrate-like AANAT (v-AANAT), instead they have insect specific GNAT (Gcn5-related *N*-acetyltransferases) that, in analogy to vertebrates, are usually called insect-type AANATs (i-AANATs). Indeed, phylogenetic analyses have shown that i-AANATs group in different clusters than v-AANATs (Barberà *et al*., 2013; Falcón *et al*., 2014; Hiragaki *et al*., 2015).

If we consider a recent study in the lepidopteran *Antheraea pernyi* (Mohamed *et al*., 2014), the present work is the second report of localisation of melatonin in the central nervous system of an insect and, to our knowledge, the first to localise melatonin in the ganglia. The aforementioned report described two pairs of melatonin immunoreactive neurons (MEL-in) in the dorsal *protocerebrum* of the lepidopteran *A*. *pernyi* (Mohamed *et al*., 2014) and two equivalent pairs of MEL-in were observed in two other Lepidoptera species used as controls in the present work (see Materials and methods). Differently from Lepidoptera, in the aphid *A*. *pisum* we have observed MEL-in neurons in the ganglia, including the SOG and the TGM, but not in the *protocerebrum* (Fig. 1). Despite the absence of melatonin neurons in the aphid brain, some of the ganglionic melatonin neurons showed axonic processes that extended into the *protocerebrum* (Fig. 1). Moreover, the end of these axons could be traced to the posterior contra-lateral neuropils in the SOG and TGM forming arborisations and varicosities. These structures resembled the primary *protocerebral* arborisations identified with PDF antibodies in *Rhodnius prolixus* by Vafopoulou *et al*. (2010) that were described as neuronal connections with dendrites of local neurons. In the pea aphid, these structures could provide input to other melatonin expressing neurons in order to elicit a coordinated response in conjunction with the clock neurons (Barberà *et al*., 2017) and/or the NSC group I found in the *pars intercerebralis* that produces a yet unidentified factor (called virginoparin) that promotes production of parthenogenetic females (Steel & Lees, 1977; Steel, 1978). Interestingly, the distribution of MEL-in in the ganglia of *A*. *pisum* was very similar to that described for NSC revealed by paraldehyde fuchsin (PAF) staining in the aphid *Megoura viciae* (Steel, 1977). The presence in *A*. *pisum* after stage L3 of numerous swellings along the axons originating from the MEL-in resembles previous observations on the distribution of neurosecretory material along the axons deriving from different *M. viciae*

NSCs (Steel, 1977). The methodology previously adopted for melatonin quantification in insects usually involved the use of radioactivity (Bembenek *et al*., 2005; Yang *et al*., 2007; Mohamed *et al*., 2014). More recently we have employed HPLC MS/MS for the quantification of melatonin in aphids, which led to two main conclusions (Escrivá *et al*., 2016). First, no significant differences in melatonin levels were found between ZT6 and ZT18 (Fig. 2A). This view contrasts with the night peak of melatonin commonly observed in other insects. However, our results agree with previous melatonin quantification in whole aphids reared under LD and SD conditions showing no significant differences between mid-photophase and mid-scotophase melatonin content (Gao & Hardie, 1997).

However, further investigations are needed as our melatonin quantification was performed in whole aphids that may include melatonin produced in other tissues apart from the head, including embryos, which could be masking a putative circadian rhythm of melatonin in the central nervous system. Moreover, the inclusion of only two time points in our experiment could have hindered the observation of a putative melatonin circadian rhythm. Additionally, it would be interesting to track the melatonin content in the LD to SD transitions.

Most interesting our quantitative analysis revealed that in the YR2 (holocyclic) strain, the level of melatonin was higher in aphids reared under SD than in those under LD conditions, while melatonin levels remained the same under both photoperiods in the GR (anholocyclic) strain (Fig. 2B). In a previous publication, melatonin levels in *A. pisum* showed a trend to be higher in LD respect to SD (Gao & Hardie, 1997). This has also been reported in *A. pernyi* (Mohamed *et al*., 2014), although in this lepidopteran, the photoperiodic response refers to the termination of diapause which is triggered by LD photoperiod, being the photoperiodic response still associated to a high melatonin content. The present melatonin

quantification analysis in aphids is the first that systematically analyses differences between photoperiods in both holocyclic (photoperiodic responsive) and anholocyclic (non-photoperiodic responsive) strains. A role for melatonin, yet to be determined, in the signalling pathway of the aphid photoperiodic response can be inferred from our results. Our results suggest that high melatonin levels could act as a token of SD photoperiod, signalling the switch to sexual progeny development. Recently, melatonin and dopamine have been postulated as antagonist partners in the photoperiodic counter of *A*. *pernyi* (Mohamed *et al*., 2014; Wang *et al*., 2015). Also in *A*. *pernyi*, melatonin and serotonin control the photoperiodic response by regulating the release/synthesis of PTTH (Wang *et al*. 2013). In the cockroach *Periplaneta americana*, melatonin has been shown to inhibit vitellogenin synthesis in the fat body, which is usually associated with ovarian development (Kamruzzaman *et al*., 2016). Additionally, Kamruzzaman *et al*. (2016) found that melatonin inhibits the expression of the genes *JHAMT* (*Juvenile Hormone Acid O-MethylTransferase*) and *FAMet* (Farnesoic Acid O-Methyltransferase) encoding enzymes involved in the synthesis of Juvenile Hormone (JH). In this context it is worth noticing that JH is known to regulate diapause incidence in several insects (Denlinger *et al*., 2012; Goodman & Cusson, 2012), in addition to its roles in the regulation of development and the control of polyphenisms.

We also investigated candidate genes to encode the enzymes that regulate the synthesis of melatonin in aphids. Our present results on AANAT genes expression agree for the most part with those reported previously (Barberà *et al*., 2013). Significant circadian rhythmicity was only detected in the expression of some of these genes even though ANOVA analysis revealed differences in levels of transcription between particular time points in other instances (see Fig. S3). These apparently contradictory results could be due to low amplitude

of an underlying circadian rhythm. Moreover, the presence of canonical E-box regulatory elements, which are usually present in the promoter region of genes under the control of the circadian effector CLOCK-CYCLE (Hardin, 2004), in the 5' region of genes encoding AANAT1, AANAT2 and AANAT3 (Fig. S5) would support their expression being controlled by the circadian clock. Thus, our results on rhythmicity in the expression of i-AANAT genes should be taken cautiously and additional experiments will be necessary to demonstrate the involvement of the circadian clock in AANAT gene expression and, eventually, in melatonin synthesis. These experiments would necessarily include a search for colocalisation of particular clock proteins and AANATs and RNAi of particular clock genes. In this respect, it is worth noting that day/night changes in AANAT expression have already been reported in *P. americana* (Bembenek *et al*., 2005) and *A. pernyi* (Mohamed *et al*., 2014) but differences in *N*-acetyltransferase activity between day and night have also been reported in other insect species. With respect to a possible involvement of (some of) the aphid AANAT genes in melatonin synthesis, it is worth noting that some of the expression profiles of these genes paralleled, to some extent, those of melatonin content. In particular, both *AANAT3* gene expression and MEL content increased in SD compared to LD conditions in the YR2 strain but not in GR aphids (see Figs. 2 and 3). A higher expression in SD than in LD was also observed for *AANAT1* and *AANAT2* genes in the YR2 and GR strains, but levels of expression were much lower in GR for *AANAT2* (see Fig. 3). Thus, the parallelism between the observed pattern of expression of *AANAT3* and, to some extent, of *AANAT2,* and the increase in melatonin levels in SD compared to LD specific to the YR2 strain, suggest, though indirectly, the participation of *AANAT2* and/or *AANAT3* in the regulation of melatonin biosynthesis. We explored this putative participation by trying to co-localise their transcripts with melatonin. Although a similar pattern of expression restricted to the SOG and the TGM

was observed between the *AANAT2* gene and melatonin, our results did not show a precise co-localisation between melatonin and *AANAT2* nor *AANAT3* (the latter being also expressed in other locations in the CNS apart from the SOG and the TGM) (Fig. 4). If any of the AANAT genes was involved in melatonin synthesis we would expect their mRNAs to be localized in the same cells where melatonin is detected unless that their encoded proteins are transported to different cells to exert their function or that different steps in the pathway of melatonin biosynthesis occur at different neurons with the final methylation step taking place in different nearby cells. The latter possibility would involve the mobilization of *N*-acetylserotonin from its place of synthesis by an insect AANAT (hypothetically AANAT2 or AANAT3) to different nearby neurons where a methyl transferase would perform the last step in the pathway to render the final melatonin. However, it is not known whether the melatonin biosynthetic pathway is conserved in insects compared to vertebrates. In vertebrates the last step in the pathway is performed by a hydroxindole-*O*-methyltransferase (HIOMT) that, however, does not have an orthologue in insects (our unpublished results) but HIOMT-immunoreactivity was detected in the MEL-in of *A. pernyi* (Mohamed *et al*., 2014) and putative HIOMT enzymatic activity was observed in *Bombyx mori* (Itoh *et al*., 1998). Thus, it is likely that the last methylation step in the pathway be performed in insects by a phylogenetically distant methyl transferase. Localization of serotonin producing neurons in the aphid CNS would undoubtedly shed light on this issue as we would expect it to co-localize with the *N*-acetyltransferase(s) responsible for its acetylation. It is worth noting here that AANATs are known to participate in different metabolic processes such as sclerotization (Zhan *et al*., 2010) or regulation of neurotransmitters (Hiragaki *et al*., 2015) among others and it is thus possible that aphid AANATs be localized at other places apart from those dedicated to MEL synthesis.

Finally, in the present report we have shown the localisation of melatonin in an insect nervous ganglion for the first time, revealing its axonic mobilization during development. Although there were no differences in the pattern of distribution of melatonin between holocyclic and anholocyclic aphids, we observed an increase in the levels of melatonin, which parallels the photoperiodic response. We showed a correlation in the expression levels of two of the four *AANAT* genes (*AANAT2* and *AANAT3*) with the levels of melatonin, although their mRNAs were not localized within MEL-in neurons. At this point, we cannot discard AANAT1 and/or AANAT4 participating in the regulation of melatonin synthesis, nor rule out a role for other enzymatic steps such as a methyl-transferase HIOMT-like. Finally, although this work opens new perspectives for the study of photoperiodism in aphids and insects in general, further work, including RNAi of aphid AANAT genes, would help to unveil the details of the melatonin biosynthetic pathway and will undoubtedly contribute to understand the role of melatonin in insect photoperiodism.

Acknowledgments

This work was supported by project CGL2015-68188-P. MB, JMCA and LE enjoyed PhD fellowships BES-2009-026077, BES-2012-052837 and BES-2014-068039, respectively from the Spanish MICINN and MINECO. ER was supported by grant BB/H018093/1 from the UK Biotechnology and Biological Sciences Research Council (BBSRC). The facilities at the Genomics, Microscopy and Greenhouse services at the SCSIE (Universitat de València) were used for sequencing, RT-qPCR, microscopy image analysis and for growing *Vicia faba* plants, respectively.

Disclosure

The authors declare that they have no conflicts of interest.

References

Barberà, M., Mengual, B., Collantes-Alegre, J.M., Cortés, T., González and A., Martínez-Torres, D. (2013) Identification, characterization and analysis of expression of genes encoding arylalkylamine N-acetyltransferases in the pea aphid *Acyrthosiphon pisum*. *Insect Molecular Biology*, 22, 623–634.

Barberà, M., Collantes-Alegre, J.M. and Martínez-Torres, D. (2017) Clock genes and photoperiodism in the aphid *Acyrthosiphon pisum*. *Insect Biochemistry and Molecular Biology*, 83, 54–67.

Bembenek, J., Sehadova, H., Ichihara, N. and Takeda, M. (2005) Day/night fluctuations in melatonin content, arylalkylamine N-acetyltransferase activity and NAT mRNA expression in the CNS, peripheral tissues and hemolymph of the cockroach, *Periplaneta americana*. *Comparative Biochemistry and Physiology - Part B: Biochemistry & Molecular Biology*, 140, 27–36.

Bradshaw, W.E. and Holzapfel, C.M. (2010) Circadian clock genes, ovarian development and diapause. *BMC Biology*, 8, 115.

Bradshaw, W.E. and Holzapfel, C.M. (2007) Evolution of animal photoperiodism. *Annual Review of Ecology*, *Evolution*, *and Systematics*, 38, 1–25.

Brömme, H.J., Peschke, E. and Israel, G. (2008) Photo-degradation of melatonin: influence of argon, hydrogen peroxide, and ethanol. *Journal of Pineal Research*, 44, 366–372.

Cazaméa-Catalan, D., Besseau, L., Falcón, J. and Magnanou, E. (2014) The timing of timezyme diversification in vertebrates. *PLoS ONE*, 9, e112380.

Cornelissen, G. (2014) Cosinor-based rhythmometry. *Theoretical Biology and Medical Modelling*, 11, 16.

Dardente, H., Wyse, C.A., Birnie, M.J., Dupré, S.M., Loudon, A.S.I., Lincoln, G.A. *et al.* (2010) A molecular switch for photoperiod responsiveness in mammals. *Current Biology*, 20, 2193–2198.

Dibner, C., Schibler, U. and Albrecht, U. (2010) The mammalian circadian timing system: Organization and coordination of central and peripheral clocks. *Annual Review of Physiology*, 72, 517–549.

Emerson, K.J., Bradshaw, W.E. and Holzapfel, C.M. (2009a) Complications of complexity: integrating environmental, genetic and hormonal control of insect diapause. *Trends in Genetics*, 25, 217–325.

Emerson, K.J., Dake, S.J., Bradshaw, W.E. and Holzapfel, C.M. (2009b) Evolution of photoperiodic time measurement is independent of the circadian clock in the pitcher-plant mosquito, *Wyeomyia smithii*. *Journal of Comparative Physiology A-Neuroethology Sensory Neural and Behavioral Physiology*, 195, 385–391.

Escrivá, L., Manyes, L., Barberà, M., Martínez-Torres, D. and Meca, G. (2016) Determination of melatonin in *Acyrthosiphon pisum* aphids by liquid chromatography-tandem mass spectrometry. *Journal of Insect Physiology*, 86, 48–53.

Falcón, J., Coon, S.L., Besseau, L., Cazaméa-Catalan, D., Fuentès, M., Magnanou, E. *et al.* (2014) Drastic neofunctionalization associated with evolution of the timezyme AANAT 500 Mya. *Proceedings of the National Academy of Sciences USA*, 111, 314–319.

Gao, N. and Hardie, J. (1997) Melatonin and the pea aphid, *Acyrthosiphon pisum*. *Journal of Insect Physiology*, 43, 615–620.

Goodman, W.G. and Cusson, M. (2012) *The Juvenile Hormones. In: Insect Endocrinology.* Elsevier, pp. 310–365.

Gorbet, D.J. and Steel, C.G.H. (2003) A miniature radioimmunoassay for melatonin for use with small samples from invertebrates. *General and Comparative Endocrinology*, 134, 193–197.

Hardeland, R. (2010) Melatonin metabolism in the central nervous system. *Current Neuropharmacology*, 8, 168–181.

Hardie, J. (1981) Juvenile hormone and photoperiodically controlled polymorphism in *Aphis fabae*: Prenatal effects on presumptive oviparae. *Journal of Insect Physiology*, 27, 257–265.

Hardin, P.E. (2004) Transcription Regulation within the Circadian Clock: The E-box and Beyond. *Journal of Biological Rhythms*, 19, 348–360.

Hiragaki, S., Suzuki, T., Mohamed, A.A.M. and Takeda, M. (2015) Structures and functions of insect arylalkylamine N-acetyltransferase (iaaNAT) a key enzyme for physiological and behavioral switch in arthropods. *Frontiers in Physiology*, 6, 1–16.

Ikegami, K. and Yoshimura, T. (2012) Circadian clocks and the measurement of daylength in seasonal reproduction. *Molecular and Cellular Endocrinology*, 349, 76–81.

Ikeno, T., Ishikawa, K., Numata, H. and Goto, S.G. (2013) Circadian clock gene *Clock* is involved in the photoperiodic response of the bean bug *Riptortus pedestris*. *Physiological Entomology*, 38, 157–162.

Ikeno, T., Numata, H. and Goto, S.G. (2011a) Photoperiodic response requires mammalian-type cryptochrome in the bean bug *Riptortus pedestris*. *Biochemical and Biophysical Research Communications*, 410, 394–397.

Ikeno, T., Numata, H. and Goto, S.G. (2011b) Circadian clock genes period and cycle regulate photoperiodic diapause in the bean bug *Riptortus pedestris* males. *Journal of Insect Physiology*, 57, 935–938.

Ikeno, T., Tanaka, S.I., Numata, H. and Goto, S.G. (2010) Photoperiodic diapause under the control of circadian clock genes in an insect. *BMC Biology*, 8, 116.

Ishikawa, A., Ogawa, K., Gotoh, H., Walsh, T.K., Tagu, D., Brisson, J.A. *et al.* (2012) Juvenile hormone titre and related gene expression during the change of reproductive modes in the pea aphid. *Insect Molecular Biology*, 21, 49–60.

Itoh, M., Hattori, A., Nomura, T., Sumi, Y., Suzuki, T., Hattori, A. *et al.* (1995) Melatonin and arylalkylamine N-acetyltransferase activity in the silkworm, *Bombyx mori*. *Molecular and Cellular Endocrinology*, 115, 59–64.

Itoh, M.T. and Sumi, Y. (1998) Melatonin and serotonin N-acetyltransferase activity in developing eggs of the cricket *Gryllus bimaculatus*. *Brain Research*, 781, 91–99.

Kamruzzaman, A., Asano, H., Hiragaki, S. and Takeda, M. (2016) Indoleamines regulate vitellogenesis via cross-talks with allatotrophe in the American cockroach, *Periplaneta americana*. *International Journal of Advanced Research*, 4, 487–497.

Klein, D.C. (2007) Arylalkylamine N-acetyltransferase, "the Timezyme". *Journal of Biological Chemistry*, 282, 4233–4237.

Lincoln, G.A. (2006) Decoding the nightly melatonin signal through circadian clockwork. *Molecular and Cellular Endocrinology*, 252, 69–73.

Linn, C.E., Poole, K.R., Roelofs, W.L. and Wu, W.Q. (1995) Circadian changes in melatonin in the nervous system and hemolymph of the cabbage looper moth, *Trichoplusia ni*. *Journal of Comparative Physiology A*, 176, 761–771.

Livak, K.J. and Schmittgen, T.D. (2001) Analysis of relative gene expression data using real-time quantitative PCR and the $2^{-\Delta\Delta CT}$ method. *Methods*, 25, 402–408.

Lucas, R.J. (2013) Mammalian inner retinal photoreception. *Current Biology*, 23, R125–R133.

Marcovitch, S. (1924) The migration of the Aphididae and the appearance of sexual forms as affected by the relative length of daily exposure. *Journal of Agricultural Research*, 27, 513–522.

Meuti, M.E., Stone, M., Ikeno, T. and Denlinger, D.L. (2015) Functional circadian clock genes are essential for the overwintering diapause of the Northern house mosquito, *Culex pipiens*. *Journal of Experimental Biology*, 218, 412–422.

Mohamed, A.A.M., Wang, Q., Bembenek, J., Ichihara, N., Hiragaki, S., Suzuki, T. *et al.* (2014) N-acetyltransferase (nat) is a critical conjunct of photoperiodism between the circadian system and endocrine axis in *Antheraea pernyi*. *PLoS ONE*, 9, e92680.

Moran, N. (1992) The evolution of aphid life cycles. *Annual Review of Entomology*, 37, 321–348.

Niva, C.C. and Takeda, M. (2003) Effects of photoperiod, temperature and melatonin on nymphal development, polyphenism and reproduction in *Halyomorpha halys* (Heteroptera: Pentatomidae). *Zoological Science*, 20, 963–970.

Niven, J.E., Graham, C.M. and Burrows, M. (2008) Diversity and evolution of the insect ventral nerve cord. *Annual Review of Entomology*, 53, 253–271.

Pavelka, J., Shimada, K. and Kostal, V. (2003) Timeless: A link between fly's circadian and photoperiodic clocks? *European Journal of Entomology*, 100, 255–265.

Pegoraro, M., Gesto, J.S., Kyriacou, C.P. and Tauber, E. (2014) Role for circadian clock genes in seasonal timing: testing the bünning hypothesis. *PLoS Genetics*, 10, e1004603.

Refinetti, R., Cornélissen, G. and Halberg, F. (2007) Procedures for numerical analysis of circadian rhythms. *Biological Rhythm Research*, 38, 275–325.

Sakamoto, T., Uryu, O. and Tomioka, K. (2009) The clock gene period plays an essential role in photoperiodic control of nymphal development in the cricket *Modicogryllus siamensis*. *Journal of Biological Rhythms*, 24, 379–390.

Saunders, D.S. (2010) Controversial aspects of photoperiodism in insects and mites. *Journal of Insect Physiology*, 56, 1491–1502.

Schindelin, J., Arganda-Carreras, I., Frise, E., Kaynig, V., Longair, M., Pietzsch, T. *et al.* (2012) Fiji: an open-source platform for biological-image analysis. *Nature Methods*, 9, 676–682.

Steel, C.G.H. and Lees, A.D. (1977) The role of neurosecretion in the photoperiodic control of polymorphism in the aphid *Megoura viciae*. *Journal of Experimental Biology*, 67, 117–135.

Steel, C.G.H. (1978) Some functions of identified neurosecretory cells in the brain of the aphid, *Megoura viciae*. *General and Comparative Endocrinology*, 34, 219–228.

Steel, C.G.H. (1977) The neurosecretory system in the aphid *Megoura viciae*, with reference to unusual features associated with long distance transport of neurosecretion. *General and Comparative Endocrinology*, 31, 307–322.

Tagu, D., Sabater-Muñoz, B. and Simon, J.-C. (2005) Deciphering reproductive polyphenism in aphids. *Invertebrate Reproduction & Development*, 48, 71–80.

The International Aphid Genomics Consortium (2010) Genome sequence of the pea aphid *Acyrthosiphon pisum*. *PLoS Biology*, 8, e1000313.

Tilden, A.R., Anderson, W.J. and Hutchison, V.H. (1994) Melatonin in two species of damselfly, *Ischnura verticalis* and *Enallagma civile*. *Journal of Insect Physiology*, 40, 775–780.

Vafopoulou, X., Terry, K.L. and Steel, C.G.H. (2010) The circadian timing system in the brain of the fifth larval instar of *Rhodnius prolixus* (Hemiptera). *Journal of Comparative Neurology*, 518, 1264–1282.

Vetting, M.W., S de Carvalho, L.P., Yu, M., Hegde, S.S., Magnet, S., Roderick, S.L. *et al.* (2005) Structure and functions of the GNAT superfamily of acetyltransferases. *Archives of Biochemistry and Biophysics*, 433, 212–226.

Vieira, R., Míguez, J.M. and Aldegunde, M. (2005) GABA modulates day-night variation in melatonin levels in the cerebral ganglia of the damselfly *Ischnura graellsii* and the grasshopper *Oedipoda caerulescens*. *Neuroscience Letters*, 376, 111–115.

Vivien-Roels, B. and Pévet, P. (1993) Melatonin: presence and formation in invertebrates. *Experientia*, 49, 642–647.

Wang, Q., Mohamed, A.A. and Takeda, M. (2013) Serotonin receptor B may lock the gate of PTTH release/synthesis in the Chinese silk moth, *Antheraea pernyi*; a diapause initiation/maintenance mechanism? *PLoS ONE*, 8, 1–13.

Wang, Q., Egi, Y., Takeda, M., Oishi, K. and Sakamoto, K. (2015) Melatonin pathway transmits information to terminate pupal diapause in the Chinese oak silkmoth *Antheraea pernyi* and through reciprocated inhibition of dopamine pathway functions as a photoperiodic counter. *Entomological Science*, 18, 74–84.

Wood, S. and Loudon, A. (2014) Clocks for all seasons: Unwinding the roles and mechanisms of circadian and interval timers in the hypothalamus and pituitary. *Journal of Endocrinology*, 222, R39–R59.

Wülbeck, C. and Helfrich-Förster, C. (2007) RNA *in situ* hybridization on *Drosophila* whole mounts. *Circadian Rhythms.* pp. 495–512.

Yamano, H., Watari, Y., Arai, T. and Takeda, M. (2001) Melatonin in drinking water influences a circadian rhythm of locomotor activity in the house cricket, *Acheta domesticus*. *Journal of Insect Physiology*, 47, 943–949.

Yang, L., Qin, Y., Li, X., Song, D. and Qi, M. (2007) Brain melatonin content and polyethism in adult workers of *Apis mellifera* and *Apis cerana* (Hym., Apidae). *Journal of Applied Entomology*, 131, 734–739.

Zhan, S., Guo, Q.H., Li, M.H., Li, M.W., Li, J.Y., Miao, X.X. *et al.* (2010) Disruption of an N-acetyltransferase gene in the silkworm reveals a novel role in pigmentation. *Development*, 137, 4083–4090.

Manuscript received August 1, 2018

Final version received November 2, 2018

Accepted November 5, 2018

Supporting Information

Table S1 List of primers used for RT-qPCR[a], PCR[b] amplification and probe synthesis[c] of the aphid *AANAT* genes.

Table S2 Templates used to synthesise RNA probes were amplified with the following primers.

Table S3 Summary of melatonin quantification by HPLC-MS/MS.

Fig. S1 Diagram summarising the induction of the seasonal response in *A. pisum* aphids. Note that sexual morphs are only obtained in holocyclic aphids of the YR2 strain under SD conditions, while those of the GR strain keep reproducing by parthenogenesis under the same SD conditions. Each of the four experiments (localisation of melatonin by IHC, quantification of melatonin by HPLC-MS/MS, localisation of *i-AANAT* transcripts by ISH, and quantification of expression of *i-AANATs* by RT-qPCR) was performed using independent induction processes. Quantification of melatonin content was obtained for the four larval stages (L1 to L4) and adult aphids of different age (1, 3, 5, 7 and 9 days after adult moult). Localisation of *i-AANAT* transcripts was carried out only in L3 and adult aphids of the YR2 strain reared under LD conditions.

Fig. S2 Z-stack confocal images of brains related to antibody specificity tests. MEl-in are indicated by white arrowheads in A and B (A) MEL-in in the brain of larval *Brithys crini*. (B) Albeit weak, 4 pairs of MEL-in are visible in the *pars intercerebralis* of late pupae *Spodoptera exigua*. (C) Aphid CNS control hybridisation without primary MEL antibody. Autofluorescence from ommatidia indicated by white arrowheads in C. Also in C note the absence of MEL signal in the SOG and TGM.

Fig. S3 Expression profiles of the *i-AANAT* aphid genes obtained for the holocyclic strain YR2 (left) and the anholocyclic strain GR (right). The expression results from aphids reared under LD (Long Day, 16 L : 8 D) are represented by black circles and those of SD (Short Day, 12 L : 12 D) by black triangles. Significant differences in expression at different time points are indicated in bold and italic letters for LD and SD photoperiods, respectively. Significant rhythmicity shown after the COSINOR analysis is indicated by red lines. The dark phase of the photoperiods is indicated as grey background ranging from ZT12 to ZT24 in SD and ZT16 to ZT24 in LD.

Fig. S4 Colocalisation of each of the i-*AANAT* transcripts and melatonin in the central nervous system of L3 aphids of the YR2 strain. For each of the genes, Z-stack confocal images showing a dorsal view of the aphid central nervous system showing the detection of transcripts (top), melatonin (center) and merge (bottom) are included in the left column, and the respective antisense probe controls in the right column. (A) *AANAT1* (blue), (B) *AANAT2* (cyan), (C) *AANAT3* (green) and (D) *AANAT4* (yellow). Although images are shown for the four *AANAT* genes, only *AANAT2* and *AANAT3* revealed positive results. Melatonin is shown in red. Bars = 50 μm.

Fig. S5 Schematic diagram of the regions upstream exon 1 of each aphid AANAT gene showing in yellow the position of canonical E-box elements (CACGTG) found after a search in the corresponding genomic regions. Approximate distance from the first exon is indicated

above each element. Assembly gaps are indicated as "gap" in white boxes. White and grey colours in exon 1 boxes indicate UTR and CDS, respectively

Figure legends

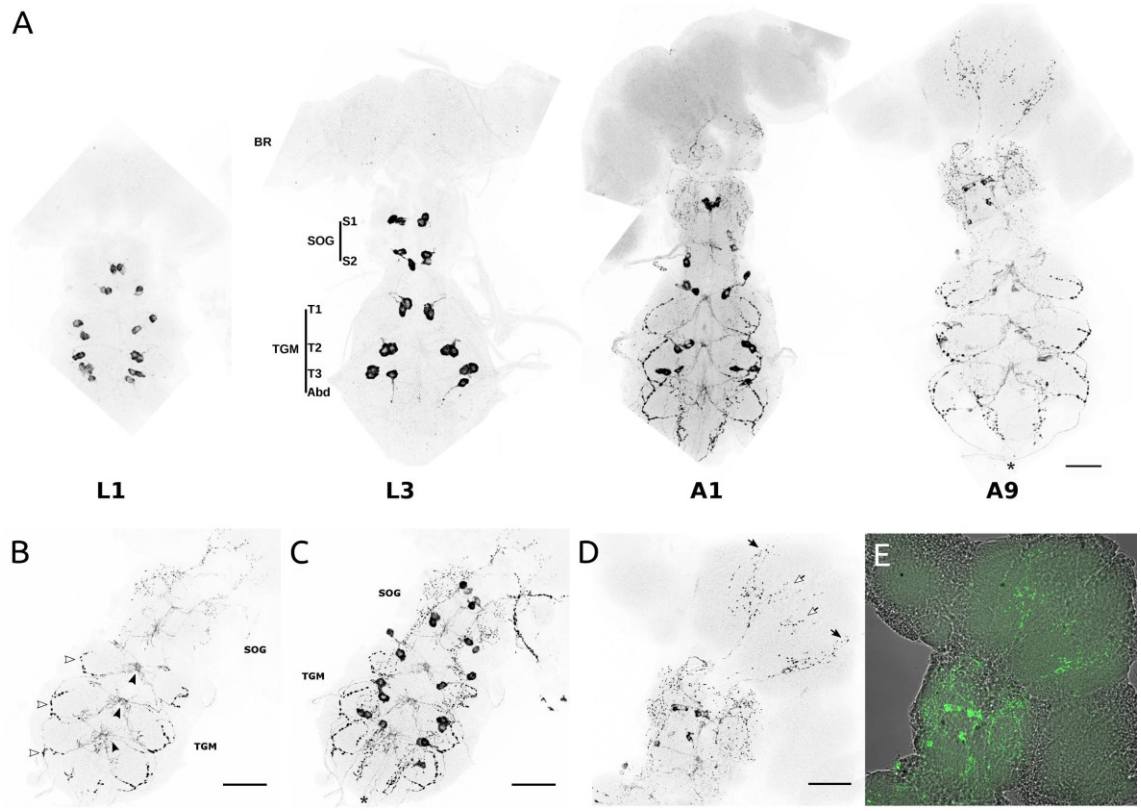

Fig. 1 Z-stack confocal images showing the localisation of MEL-in in the pea aphid CNS. (A) Comparison of MEL in CNSs of YR2 aphids at different developmental stages. L1 and L3 correspond to larval stages 1 and 3, respectively. A1 and A9 correspond to aphids of 1 and 9 days since last moult to adult stage. A general view of MEL positive neurons and their distribution in the aphid CNS is shown in the L3 preparation. (B) Z-stack including the most ventral image slices of the aphid nervous ganglia. The tree ventro-medial commissures are indicated by full arrowheads and the three arc-shaped axons are indicated by empty arrowheads. (C) Same preparation as B but including the complete Z-stack. (D) Detail of the protocerebral MEL arborised axons. Empty arrows indicate tritocerebral branches. Full arrows indicate branches reaching pars lateralis. (E) Same as D showing MEL in green merged with a light microscopy image of the same brain. Black and white values were inverted, except for E. Asterisks indicate the beginning of the posterior nerve. BR, brain; SOG, suboesophageal ganglion; TGM, thoracic ganglionic mass; S1 and S2 refer to the first and second SOG neuromeres; T1-T3 refer to the first, second and third TGM neuromeres, respectively; Abd refers to fused abdominal ganglia; L1 and L3 refer to first and third larval stage aphids; A1 and A9 refer to one and nine days old adult aphids. Bars = 50 μm.

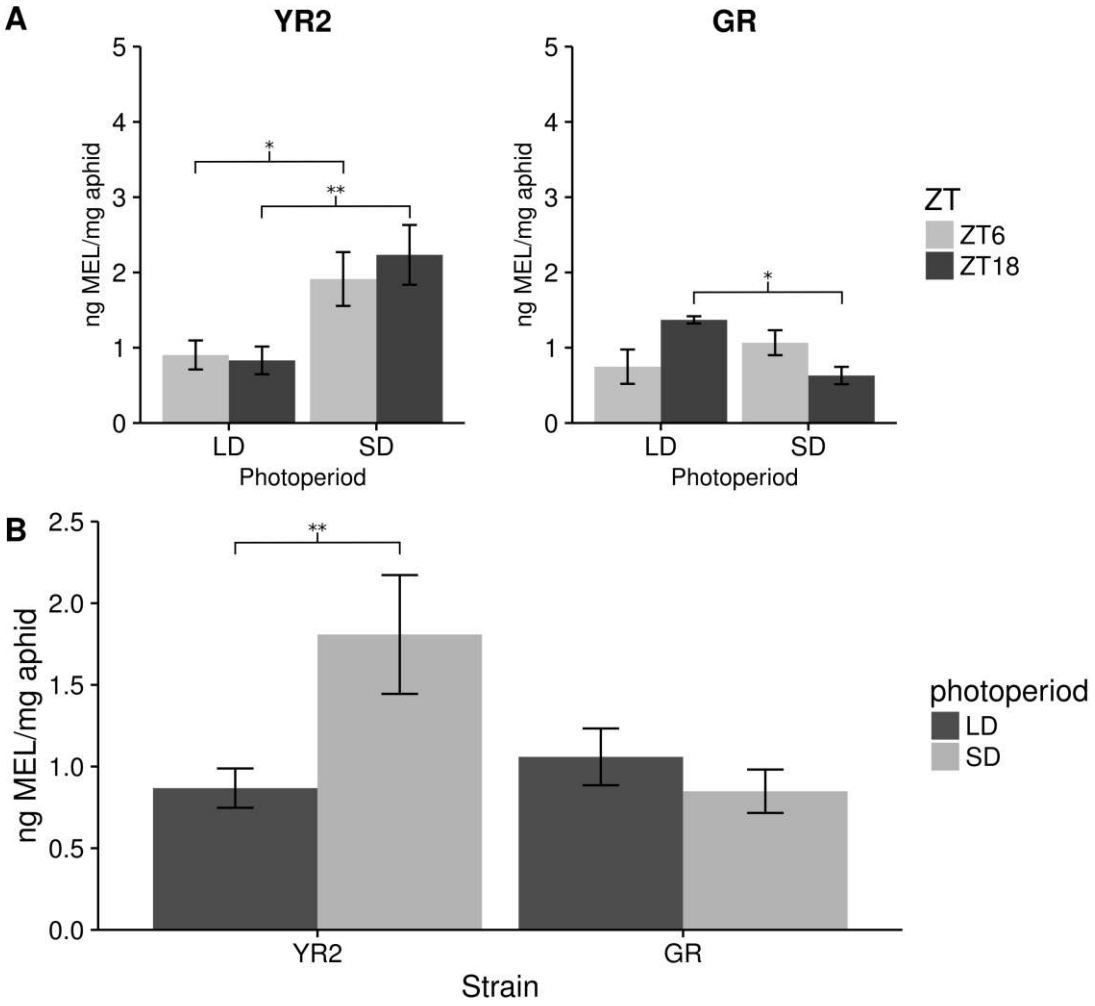

Fig. 2 Analysis of MEL quantification in aphids. Bars represent the mean MEL content ± SEM. (A) Comparison of MEL content at ZT6 and ZT18 in aphids of the holocyclic strain YR2 (left) and the anholocyclic strain GR (right) reared under two different photoperiods. (B) Comparison of global MEL content in aphids of the YR2 and GR strains reared under LD and SD photoperiods. ANOVA significant *P*-values are indicated by **P* < 0.05, ***P* < 0.001.

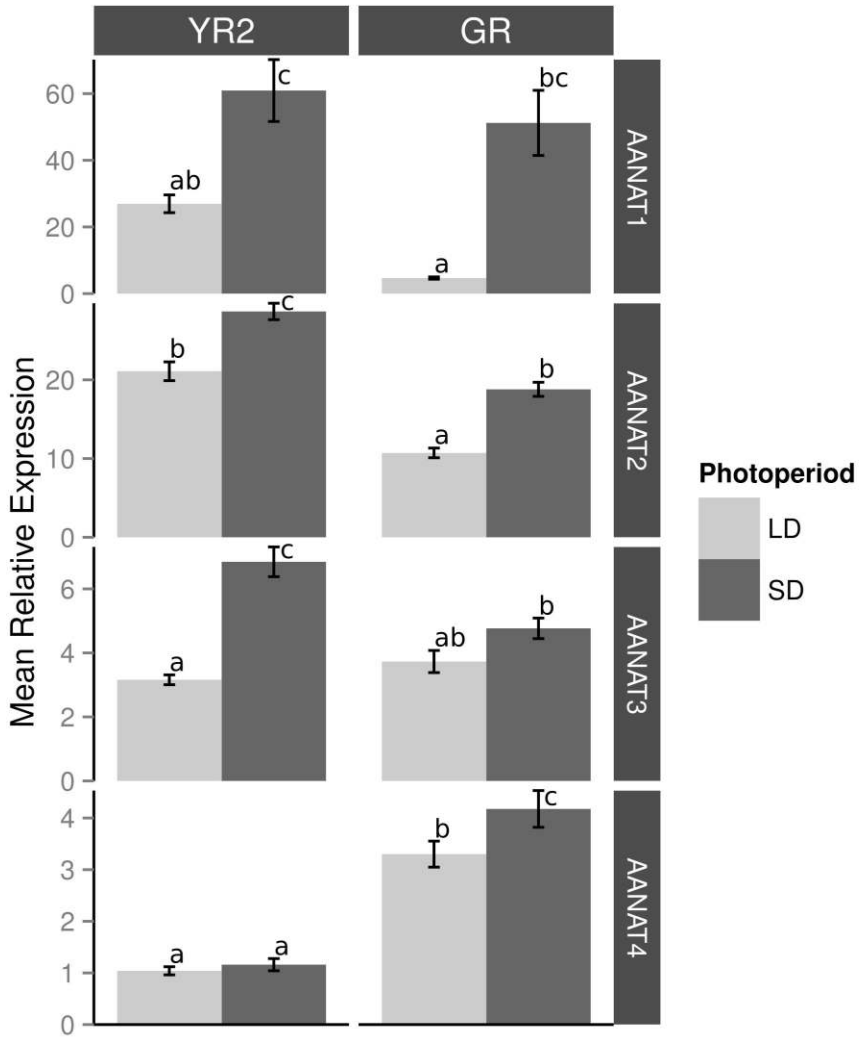

Fig. 3 Comparison of levels of expression of the i-*AANAT* genes between aphid strains and photoperiods. Bars represent the mean relative expression calculated for all ZT within a strain and photoperiod ± SEM. Letters on top of each bar represent the subgroup significance ($P < 0.05$) of the ANOVA test comparing the variable photoperiod for each gene.

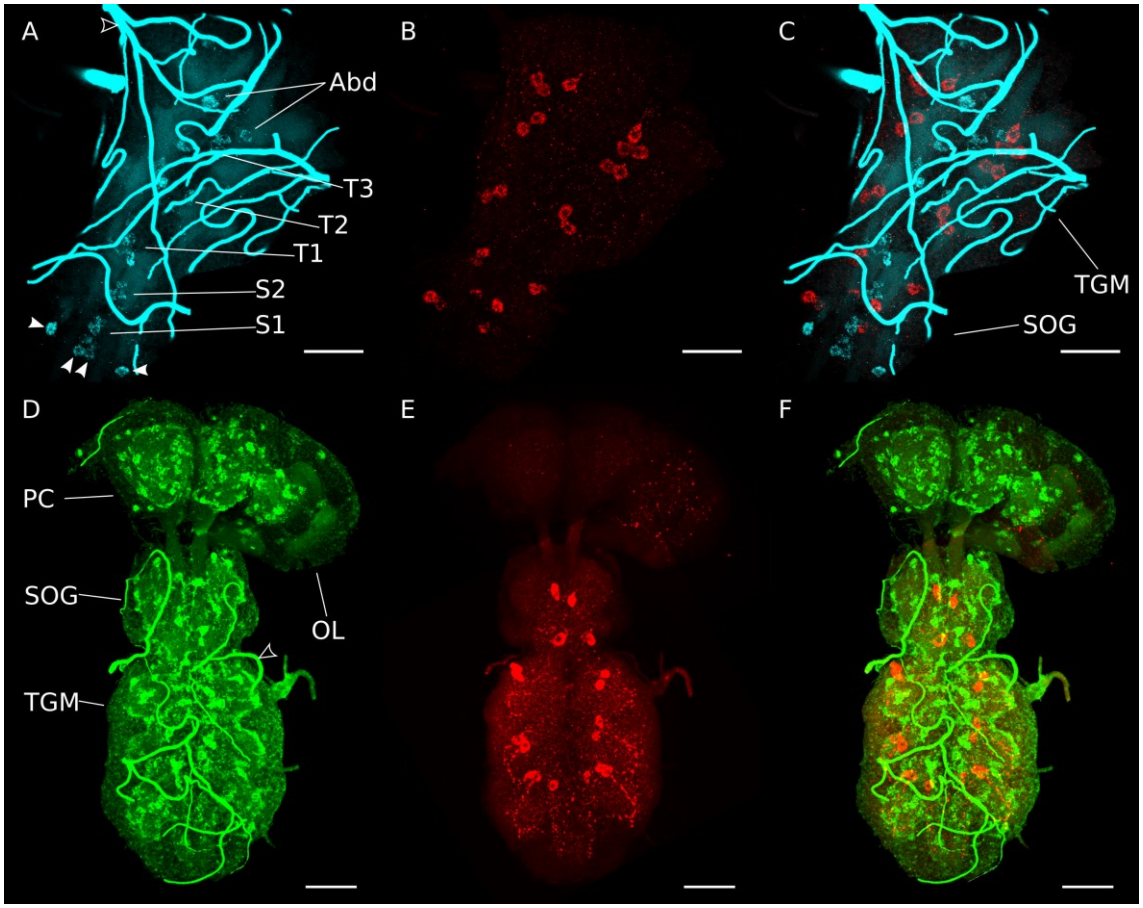

Fig. 4 Localisation of i-*AANAT* transcripts in the central nervous system of adult aphids of the YR2 strain. Z-stack confocal images showing a dorsal view of the aphid central nervous system. (A) Localisation of *AANAT2* transcripts in the nervous ganglia in cyan. Arrowheads indicate the strongly stained neurons expressing *AANAT2* located ventrally with respect to the rest of neurons. (B) Same ganglia as A showing in red the melatonin immunoreactive neurons (MEL-in). (C) A and B merged. Note the different position of *AANAT2* expressing neurons and MEL-in. (D) Localisation of *AANAT3* transcripts in the nervous ganglia in green. (E) Same central nervous system as D showing in red the MEL-in. (F) D and E merged. Note the different positions of *AANAT3* expressing neurons and MEL-in. Two empty arrowheads in A and D point to unspecific tracheal staining. Abd, abdominal neuromere; OL, optic lobe; PC, protocerebrum; SOG, suboesophageal ganglion; S1 and S2, first and second SOG neuromeres respectively; TGM, thoracic ganglionic mass; T1-T3, pro-, meso- and metathoracic neuromeres respectively. Bars = 50 μm